Online Reconstruction and Motion Detection in HARDI

E. Caruyer[1], I. Aganj[2], C. Lenglet[3], G. Sapiro[2], and R. Deriche[1]
[1]Athena Project-Team, INRIA Sophia Antipolis - Méditerranée, Sophia Antipolis, France, [2]Department of Electrical and Computer Engineering, University of Minnesota, Minneapolis, MN, United States, [3]Department of Radiology - CMRR, University of Minnesota Medical School, Minneapolis, MN, United States

Introduction: With acquisition protocols such as high angular resolution diffusion imaging, head motion can become an issue. Although the misalignment between diffusion-weighted images (DWIs) can be corrected in a post-processing step [1,2], this might increase partial volume effects, because of the relatively low spatial resolution of DWIs and interpolation in the registration procedure. If able to detect motion online, the scanner technician could be issued a warning and make a decision accordingly. Orientation distribution functions (ODF) [3] can be reconstructed online using a Kalman filter (KF) [4]. We present three contributions related to the problem of online ODF reconstruction and motion detection in HARDI. First, we develop a proper error propagation accounting for the non-linear transform on the diffusion signal. Next, we develop two motion detection algorithms, based on the monitoring of residuals, and compare them using synthetic data.

Methods:

1. Incremental reconstruction of the constant solid angle ODF Under the assumption of a mono-exponential decay of the diffusion signal, the ODF can be obtained as $\psi(\mathbf{u}) = \frac{1}{4\pi} + \frac{1}{16\pi^2}\mathrm{FRT}\left\{\nabla_b^2 \ln(-\ln\frac{S(q\mathbf{u})}{S(\mathbf{q}=\mathbf{0})})\right\}$ (1), where FRT is the Funk-Radon transform and ∇_b^2 the Laplace-Beltrami operator [3], which have closed-form matrix expressions $\mathbf{F}$ and $\mathbf{L}$ in the spherical harmonics (SH) basis defined in [6]. If we express the transformed signal $y = \ln(-\ln S/S(\mathbf{0}))$ in this basis, Eq.1 becomes $\hat{\mathbf{c}} = \frac{1}{2\sqrt{\pi}}\mathbf{e_1} + \frac{1}{16\pi^2}\mathbf{FLc}$, where $\hat{\mathbf{c}}$ and $\mathbf{c}$ are the SH coefficients describing ψ and y. The estimation of $\mathbf{c}$ from a series of measurements $y[k] = \ln\left(-\ln\frac{S[k]}{S(\mathbf{0})}\right),\ k = 1\ldots N$, is done by minimizing $M(\mathbf{c}) = (\mathbf{y}-\mathbf{Bc})^{\mathrm{T}}\boldsymbol{\Sigma}^{-1}(\mathbf{y}-\mathbf{Bc}) + \lambda\mathbf{c}^{\mathrm{T}}\mathbf{Lc}$, where $\mathbf{B}$ is the SH design matrix, $\boldsymbol{\Sigma}$ is the covariance matrix of the observation, and the second term is a regularization constraint. This is minimized incrementally using the KF (Eq. 2).

$$\begin{cases} \hat{\mathbf{c}}[0] &= \mathbb{E}[\mathbf{c}[0]] \\ \hat{\mathbf{P}}[0] &= \mathbb{E}[(\mathbf{c}-\hat{\mathbf{c}}[0])(\mathbf{c}-\hat{\mathbf{c}}[0])^{\mathrm{T}}] \\ \mathbf{P}[0] &= (\hat{\mathbf{P}}_0^{-1} + \lambda\mathbf{L})^{-1} \\ \mathbf{P}[k] &= (\mathbf{I} - \mathbf{g}[k]\mathbf{B}[k])\,\mathbf{P}[k-1] \\ \mathbf{V}[k] &= \mathbf{B}[k]\mathbf{P}[k-1]\mathbf{B}[k]^{\mathrm{T}} + \sigma^2[k] \\ \mathbf{g}[k] &= \mathbf{P}[k-1]\mathbf{B}[k]^{\mathrm{T}}\mathbf{V}[k]^{-1} \\ \gamma[k] &= y[k] - \mathbf{B}[k]\mathbf{c}[k-1] \\ \mathbf{c}[k] &= \mathbf{c}[k-1] + \mathbf{g}[k]\gamma[k] \end{cases} \quad (2)$$

2. Propagation of uncertainty: The $\sigma^2[k]$ in Eq. 2 account for the uncertainty in the diffusion weighted measurements, and for the distortion introduced by the non-linear transform. Through first order propagation of uncertainty, we have $\sigma^2[k] = \frac{\mathrm{Var}(S[k])}{S[k]^2\ln^2(S[k]/S(\mathbf{0}))}$.

3. Motion detection: We assume that the effects induced by a motion at time θ can be summarized locally as a change $\mathbf{p}$ (called jump) in the vector $\mathbf{c}$ of SH coefficients at a given voxel. Consequently, the prediction error for subsequent iterations of the KF will no longer be zero-mean. The residuals can be decomposed [6] as $\gamma[k] = \mathbf{G}(k,\theta)\mathbf{p} + \gamma_1[k]$ (3),where γ_1 is zero-mean, with covariance $\mathbf{V}[k]$. $\mathbf{G}(k,\theta)$ represents the propagation of a jump occurring at time θ to the prediction error at time k, and can be pre-computed [6].

Motion detection can be achieved by monitoring the residuals either through a *direct* approach, without any delay, or through a method based on a generalized likelihood ratio test (*GLRT*). The former estimates the mean squared value of the jump $\mathbf{p}$ over the whole volume and thresholds it to detect motion. The later relies on Eq. 3, which is a system of linear equations between the residuals $\gamma[k]$ and the jump $\mathbf{p}$. Provided that we have sufficient observations since the motion occurred, and an estimate of θ, we can estimate $\mathbf{p}$ through weighted least squares, which is the maximum likelihood estimate, as all relevant densities are Gaussian. Precisely, the maximum value of the likelihood is a good candidate for a motion detection criterion.

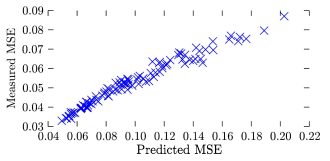

Fig.1: Compared predicted and reconstructed MSE

Results and Discussion:

On demand reconstruction accuracy We tested the KF on a set of 100 synthetic diffusion propagators, generated using a multi-tensor model, for 1-, 2- and 3-tensors, with trace and FA typical of white matter diffusivity. We estimated the MSE of $\hat{\mathbf{C}}$, and compared it to the trace of the covariance matrix $\mathbf{F}^{\mathrm{T}}\mathbf{L}^{\mathrm{T}}\mathbf{PLF}$, where $\mathbf{P}$ is given by the KF. The results of Monte-Carlo simulations for 1000 repetitions are presented on Fig.1. First, it appears that the reconstruction accuracy is highly variable from one diffusion propagator to another: the reconstruction accuracy depends on the diffusion properties. Moreover, the predicted MSE is strongly correlated to the empirical MSE. This index given by the KF with a proper propagation of noise is a powerful indicator, computed online, for the quality of the reconstructed ODF.

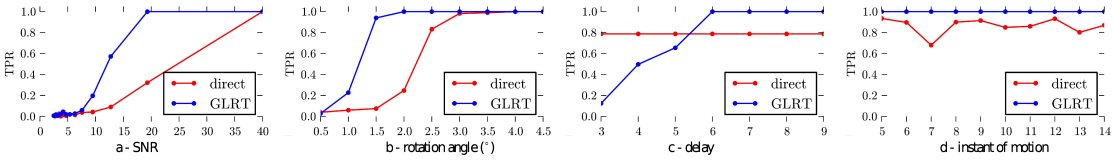

Fig.2: Motion detection, sensitivity for FPR=5%

Motion detection We have simulated the formation of DWIs, with motion occurring during acquisition. We first fit a HARDI profile at each voxel from a series of 200 DWIs of a still subject, acquired on a 3T Siemens scanner, with 200 encoding directions, b=1000 s/mm^2, 25 b=0 s/mm^2 images and 2mm isotropic voxels. For the rigid transform of interest, we extract the rotation component and apply it locally to the diffusion signal. From the baseline image, and the rotated diffusion signal, we synthesize DWIs on which we apply the rigid transform. Finally, we corrupt them by Rician noise. For repeated simulations, we estimate the true positive rate (TPR), for a false positive rate (FPR) maintained lower than 5%. The results (Fig.2) are for a rotation of 3°, occurring at instant θ=20, for SNR=20, and allowing a delay of 10 iterations. As expected, GLRT is more robust to noise, and performs better in detecting small motions, since it is calculated from a series of residuals. We can also detect motion occurring at the very beginning of a diffusion MRI acquisition: this is a consequence of the memory implemented in the calculation of the likelihood ratio. We find that the direct approach is slightly less sensitive in noisy conditions, but can still detect motion. Because of its low delay, we suggest to use it in parallel with the GLRT.

Acknowledgements: This work was partly funded by NIH (grants R01 EB008432, R01 EB007813, P41 RR008079, P30 NS057091), the University of Minnesota Institute for Translational Neuroscience, and the Computational Diffusion MRI (CD-MRI) INRIA Associate Team program.

References : [1] Rohde et al, Magn Reson Med, 51(1):103-114 [2] Barmpoutis et al, MICCAI 2007 :908-915 [3] Aganj et al, Magn Reson Med, 64(2):554-566 [4] Deriche et al, Med Image Anal, 13(4) :564-579 [5] Descoteaux et al, Magn Reson Med, 58(3) :497-510 [6] Willsky et al, Automatic Control, 21(1) :108-112